

**Native point defect energetics in GaSb: Enabling  $p$ -type conductivity of undoped GaSb**

Ville Virkkala, Ville Havu, Filip Tuomisto, and Martti J. Puska

*COMP Department of Applied Physics, Aalto University, P.O. Box 11100, FIN-00076 Aalto, Finland*

(Received 8 May 2012; revised manuscript received 28 August 2012; published 1 October 2012)

The energetics of native point defects in GaSb is studied using the density-functional theory within the hybrid functional scheme (HSE06). Our results indicate that the  $\text{Ga}_{\text{Sb}}$  antisite has the lowest formation energy and could thus be the acceptor defect responsible for the  $p$ -type conductivity of undoped GaSb. We find also that the  $\text{Sb}_{\text{Ga}}$  antisite has a remarkably low formation energy in Sb-rich growth conditions and it should act as a donor for all Fermi level positions in the band gap. However, we suggest that the structural metastability of the  $\text{Sb}_{\text{Ga}}$  antisite or extrinsic point defects, namely carbon and in particular oxygen, may neutralize its compensating character.

DOI: [10.1103/PhysRevB.86.144101](https://doi.org/10.1103/PhysRevB.86.144101)

PACS number(s): 61.72.J-, 71.55.Eq, 71.15.Nc

**I. INTRODUCTION**

Native defects and unintentional impurities introduced during the growth of compound semiconductors often cause the material to turn to a  $p$  or  $n$ -type. Via compensation, these defects may also hinder crucially the doping of the semiconductor materials. Specially GaSb, which is an important material from both material and device points of views, is always  $p$ -type when undoped.<sup>1</sup> The technological importance of GaSb stems from the fact that it can be used as a substrate material for other ternary and quaternary III-V compounds whose band gaps cover a wide spectral range from 0.8 to 4.3  $\mu\text{m}$  (Ref. 1). GaSb also shows a lot of potential as the optically active material in various optoelectronic devices<sup>1</sup> and recently it has attained a lot of attention in vertical-external-cavity surface emitting lasers.<sup>2</sup> The usefulness of GaSb is enhanced by the fact that its direct band gap can be significantly narrowed by replacing Sb with just a small fraction (around 1%) of nitrogen.<sup>3,4</sup>

The origin of the  $p$ -type conductivity of the undoped GaSb has been debated. It is often connected to Ga antisites or vacancies.<sup>1</sup> For example, based on positron lifetime studies, Ling *et al.*<sup>5</sup> concluded that most likely the existence of  $\text{Ga}_{\text{Sb}}$  antisites resulted in the  $p$ -type behavior whereas Ga vacancies could not be the cause. This identification was motivated also by the results of the density-functional theory (DFT) electronic structure calculations by Hakala *et al.*<sup>6</sup> which showed that  $\text{Ga}_{\text{Sb}}$  acts clearly as the most important acceptor from the Ga-rich growth conditions far to the Sb-rich stoichiometry. On the other hand, Peles *et al.*<sup>7</sup> suggested on the basis of DFT calculations that interstitial hydrogen would act as a shallow acceptor in GaSb.

Native point defects in GaSb have been studied extensively by Hakala *et al.*<sup>6</sup> within the DFT framework. They used the local density approximation (LDA), norm-conserving pseudopotentials, and the plane-wave expansion for electron wave functions and densities. The  $\text{Ga}_{\text{Sb}}$  antisite and the Ga interstitials were found as the most important acceptor- and donor-type defects, respectively. The abundances of the acceptor-type Ga vacancy and the electrically nonactive (existing only in the neutral charge state)  $\text{Sb}_{\text{Ga}}$  antisite were predicted as significant only for very Sb-rich growth conditions.

Despite the high expectations for the usage of GaSb it has been the subject of a relatively small number of computational

studies in comparison with other III-V compounds, especially GaAs. This motivates us to revisit the defect problematics of GaSb, especially in terms of the source of the  $p$ -type conductivity in GaSb with the help of state-of-the-art computational methods. In contrast to the earlier DFT approaches used, the state-of-the-art methods can tackle the problem of the underestimation of the band gap in the (semi)local approximations for the electron exchange and correlation and they correct more accurately for the spurious electrostatic defect-defect interactions in the supercell approximation. Both of the problems can affect the accurate calculation of the defect ionization level positions as well as the defect formation energies.<sup>8</sup> More specifically, we use a hybrid exchange-correlation functional which substitutes a portion of the semilocal exchange by the nonlocal Hartree-Fock (HF) exchange. The hybrid functionals allow one to adjust the band gap to the experimental value giving a straightforward scheme to predict the energetics of the different charge states for different Fermi level positions within the band gap. To overcome the finite-size effects due to the periodic repetition of a charged supercell we use the method by Freysoldt *et al.*<sup>9</sup> The reliable treatment of the finite-size effects is especially important when using the hybrid functionals because, at the moment, their computational expense does not allow the use of large supercells of more than  $\sim 200$  atoms. Recently, Komsa and Pasquarello<sup>10</sup> assessed the accuracy of hybrid functionals with a finite-size correction approach in the case of the  $\text{As}_{\text{Ga}}$  antisite in GaAs. They found that the hybrid functionals tuned to give the experimental band gap reproduce the experimental ionization level positions within  $\sim 0.2$  eV. This gives credence to our application of these methods in the case of native defects in GaSb.

In the present work, we found, in agreement with the results by Hakala *et al.*,<sup>6</sup> that  $\text{Ga}_{\text{Sb}}$  antisites are energetically the most favored acceptor defects, especially for Ga-rich growth conditions. However, in sharp contrast, we find that  $\text{Sb}_{\text{Ga}}$  antisites exhibit donor states  $2+$  and  $1+$  in the band gap and that consequently their formation energies in  $p$ -type materials are low. The existence of the  $\text{Sb}_{\text{Ga}}$  donor levels is in line with the (computational) findings for anion antisite defects in other III-V compound semiconductors, notably in GaAs (Refs. 10 and 11) but very interestingly also in AlSb (Ref. 12). The prediction of the  $\text{Sb}_{\text{Ga}}$  donor levels associated with low defect formation energies is a challenge for explaining the

origin of the  $p$ -type conductivity of GaSb. We found that  $\text{Sb}_{\text{Ga}}$  exhibits also a metastable  $C_{3v}$ -symmetry configuration which is similar to the EL2 defect in GaAs (see, e.g., Ref. 11) and is also predicted to exist in other III-V compounds [e.g., in AlSb (Ref. 12)]. The  $C_{3v}$  configuration is neutral for the whole range of the Fermi level in the band gap. Below we discuss the transition of the  $\text{Sb}_{\text{Ga}}$  antisite to this electrically inactive state.

Even though our main focus is on the native point defects, we also perform a very limited study of extrinsic point defects, namely carbon at the substitutional Sb site and oxygen at the interstitial cation site as possible sources of  $p$ -type conductivity. Erhart *et al.*<sup>13</sup> studied these defects in AlSb and found them as the most detrimental impurities that can be unintentionally incorporated during the growth process. They used the LDA functional and 64-atom supercell to study various extrinsic point defects in AlSb and found that substitutional carbon at the Sb site acts as a singly acceptor for the whole range of the Fermi level. Oxygen at the interstitial cation site was shown to act as a single or double acceptor with a notably low formation energy. In this paper we show that oxygen and carbon act also as acceptors in GaSb and could thus compensate the donor character of the  $\text{Sb}_{\text{Ga}}$  antisite.

The organization of the present paper is as follows. The computational methods with parameters chosen and benchmark results obtained are given in Sec. II. Section III presents the energetics and geometries of the different native defects in GaSb and those of the carbon and oxygen impurities. The implications of the results are discussed in Sec. IV and Sec. V is a short summary.

## II. METHODS

All the present calculations are performed using the Vienna *ab initio* simulation package (VASP)<sup>14</sup> with the projector augmented wave (PAW)<sup>15</sup> method. The HSE06 hybrid functional<sup>16</sup> is used except in some test and reference calculations where the LDA functional is employed. For the default HF mixing constant of 25% the obtained lattice constant is 6.16 Å and the band gap is 0.64 eV. However, we adjust the mixing constant to reproduce the experimental band gap of 0.81 eV at 0K. This is a commonly recommended procedure when hybrid functionals are used in defect calculations.<sup>10,17</sup> The adjusted HF mixing constant is 29% and the corresponding lattice constant 6.15 Å, which is somewhat larger than the experimental value of 6.10 Å (Ref. 18.) We use the plane-wave cutoff energy of 300 eV which provides a good convergence of the total energy. For the HSE range separation parameter  $\mu$  we use the value 0.2/Å. All the calculations are performed in a 64-atom simple cubic supercell and the  $2 \times 2 \times 2$  Monkhorst-Pack set is used for the  $\mathbf{k}$ -point sampling in most of the cases. The few exceptions are explained in more detail below. Atoms are relaxed to their ground-state positions without any symmetry restrictions. The stopping criterion for ionic relaxation is that the total force acting on each atom is less than 0.02 eV/Å in magnitude. All the cases are calculated as spin polarized.

The studied systems are Ga ( $V_{\text{Ga}}$ ) and Sb ( $V_{\text{Sb}}$ ) vacancies, Ga and Sb interstitials at the hexagonal ( $H$ ) site and at the tetrahedral sites ( $T_c, T_a$ ), and Ga ( $\text{Ga}_{\text{Sb}}$ ) and Sb ( $\text{Sb}_{\text{Ga}}$ ) antisites. At the  $T_a$  interstitial site the defect has four anions and at the

$T_c$  interstitial site four cations as nearest neighbors. We also studied two Sb atoms sharing one Sb site, Sb split-interstitial  $[(\text{Sb-Sb})_{\text{Sb}(110)}]$ , oriented along the  $\langle 110 \rangle$  direction, which is reported to have a rather low formation energy in AlSb (Ref. 19). The extrinsic point defects studied in this work are carbon at the substitutional Sb site ( $C_{\text{Sb}}$ ) and oxygen at the interstitial cation site  $[\text{O}(T_c)]$ . These extrinsic point defects are chosen because they act as acceptors in AlSb and their formation energies were found to be the lowest ones for carbon and oxygen impurities in AlSb (Ref. 13).

To overcome the finite-size effects due to periodic repetition of the net defect charge  $q$  we use the method by Freysoldt *et al.*<sup>9</sup> The defect charge distribution  $q_d(\mathbf{r})$  is approximated by a Gaussian of  $1 a_0$  in width and for the macroscopic high-frequency dielectric constant  $\epsilon$  of GaSb the experimental value of 14.4 (Ref. 20) is used. For unrelaxed supercells the potential alignment constant  $C$ , needed to align the energy levels of the defect and bulk supercells, can be determined visually.<sup>9</sup> However, in the case of relaxed supercells this method cannot be directly used because the nuclei in the defect supercell move relative to their positions in the bulk supercell and, thus, the changes in ionic potentials completely swamp the underlying defect potential. That is why in this work  $C$  is determined by calculating the potential difference between the defect and bulk supercells at a point far from the defect and subtracting the periodic long-range potential  $\tilde{V}_q^{lr}(\mathbf{r}_{\text{far}})$  of the defect charge distribution at this point from the difference, that is,

$$C = \tilde{V}_{\text{defect}}(\mathbf{r}_{\text{far}}) - \tilde{V}_{\text{bulk}}(\mathbf{r}_{\text{far}}) - \tilde{V}_q^{lr}(\mathbf{r}_{\text{far}}). \quad (1)$$

Above,  $\tilde{V}_{\text{defect}}(\mathbf{r}_{\text{far}})$  and  $\tilde{V}_{\text{bulk}}(\mathbf{r}_{\text{far}})$  are the electrostatic potentials far from the defect in the defect and bulk supercells, respectively.

The defect formation energies for intrinsic defects are calculated using the formula<sup>21</sup>

$$E^f = E_{\text{tot}}[\text{def} + \text{bulk}] - E_{\text{tot}}[\text{bulk}] - n_{\text{Ga}}\mu_{\text{Ga}} - n_{\text{Sb}}\mu_{\text{Sb}} + q(E_v + E_f) - \Delta E, \quad (2)$$

where  $E_v$  is set equal to the valence band maximum (VBM),  $E_f$  is the Fermi level referenced to the valence band maximum,  $\mu_{\text{Ga}}$  and  $\mu_{\text{Sb}}$  are the chemical potentials of the Ga and Sb atoms, respectively. Further,  $n_{\text{Ga}}$  and  $n_{\text{Sb}}$  are the numbers of the removed (a negative number) or added (a positive number) Ga and Sb atoms, respectively, and  $\Delta E$  is the energy correction term<sup>9</sup>

$$\Delta E = \frac{2\pi}{\epsilon\Omega} \sum_{\mathbf{G} \neq 0}^{|\mathbf{G}| \leq G_{\text{cut}}} \frac{q_d(|\mathbf{G}|)^2}{|\mathbf{G}|^2} - \frac{1}{\pi\epsilon} \int_0^{G_{\text{cut}}} q_d(g)^2 dg + qC. \quad (3)$$

In the above,  $q_d(g)$  is the model charge distribution in the reciprocal space,  $\Omega$  is the supercell volume, and  $G_{\text{cut}}$  is an appropriately chosen cutoff radius ensuring convergence of the correction term. In Ga (Sb)-rich growth conditions  $\mu_{\text{Ga}}$  ( $\mu_{\text{Sb}}$ ) is equal to that of  $\mu_{\text{Ga}[\text{bulk}]}$  ( $\mu_{\text{Sb}[\text{bulk}]}$ ) and in Sb (Ga)-rich growth conditions  $\mu_{\text{Ga}}$  ( $\mu_{\text{Sb}}$ ) is obtained as  $\mu_{\text{Ga}} = \mu_{\text{GaSb}} - \mu_{\text{Sb}[\text{bulk}]}$  ( $\mu_{\text{Sb}} = \mu_{\text{GaSb}} - \mu_{\text{Ga}[\text{bulk}]}$ ), where  $\mu_{\text{GaSb}}$  is the energy of the two-atom unit of bulk GaSb (Ref. 21). The chemical potentials for bulk Ga and Sb are calculated in their point symmetries  $\text{Cmca}$  and  $\text{R}\bar{3}\text{m}$ , respectively. The comparison of the calculated enthalpy of formation for GaSb

$\Delta H = \mu_{\text{GaSb}} - \mu_{\text{Ga[bulk]}} - \mu_{\text{Sb[bulk]}} = -0.46$  eV, with the experimental value of  $-0.43$  eV (Ref. 22), serves also as a benchmark test for our DFT calculations.

In calculating the formation energies for the impurity defects we need to add the term<sup>13</sup>

$$-\sum_i^{imp} \Delta n_i (\mu_i^{\text{bulk}} + \Delta\mu_i) \quad (4)$$

into Eq. (2), where  $\Delta n_i$  denotes the difference in the number of impurity atoms  $i$  between the bulk and defect supercells,  $\mu_i^{\text{bulk}}$  is the chemical potential of impurity  $i$  in its reference state, and  $\Delta\mu_i$  is the change in the chemical potential of this impurity with respect to bulk chemical potential. The chemical potential  $\mu_i^{\text{bulk}}$  is calculated in the most stable phase for the impurity (graphite for C and O<sub>2</sub> for O) and  $\Delta\mu_i$  is set to zero. We also found it necessary to increase the energy cutoff radius of the plane-wave basis set to 400 eV in the case of extrinsic point defects.

The sources of errors within the used DFT framework are related to the  $\mathbf{k}$ -point sampling and to the finite-size effects due to limited supercell size. On the basis of the the test calculations with the  $4 \times 4 \times 4$   $\mathbf{k}$ -point sampling we estimate the  $\mathbf{k}$ -point sampling error for the relevant defects to be  $< 0.1$  eV. However, for the neutral Sb antisite in the  $T_d$  and  $C_{3v}$  configurations and for the Sb vacancy in the  $-1$  charge state we found it necessary to use the  $4 \times 4 \times 4$   $\mathbf{k}$ -point sampling for the DFT part. The ionic relaxations were made similarly to the other cases. Using the LDA functional, we have studied the convergence of the formation energy with respect to supercell size in the case of Ga vacancies in charge states from 0 to  $-3$ . We found that for all charge states the formation energies have converged better than 0.2 eV.

### III. RESULTS

#### A. Ionization levels and ionic configurations for native point defects

Figure 1 shows the different charge states and the ensuing ionization levels for the different vacancy and antisite defects in GaSb. The level positions are based on the numerical data given in Table I. The Ga vacancy is stable in the charge states from 0 to  $-3$ . These charge states were found also for the Ga vacancy in GaAs in hybrid functional calculations by Komsa and Pasquarello.<sup>23</sup> The only difference is that now the

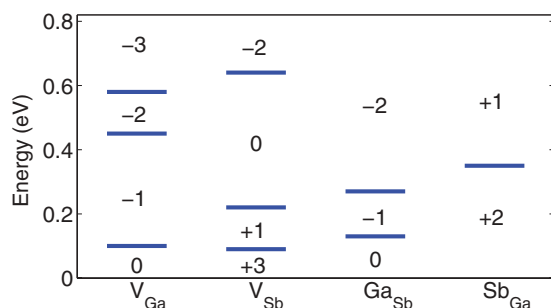


FIG. 1. (Color online) Calculated stability regions of different charge states and the ensuing ionization levels for vacancies and antisites in GaSb.

TABLE I. Calculated formation energies of the stable vacancy, antisite, and interstitial defects in GaSb in Ga-rich and Sb-rich growth conditions corresponding to the Fermi level at the VBM.

Defect	$E_f$ (eV) Ga rich	$E_f$ (eV) Sb rich
$V_{\text{Ga}}^{3-}$	4.10	3.63
$V_{\text{Ga}}^{2-}$	3.52	3.05
$V_{\text{Ga}}^{1-}$	3.07	2.60
$V_{\text{Ga}}^0$	2.97	2.50
$V_{\text{Sb}}^{2-}$	4.31	4.78
$V_{\text{Sb}}^0$	3.03	3.50
$V_{\text{Sb}}^{1+}$	2.81	3.27
$V_{\text{Sb}}^{3+}$	2.63	3.10
$\text{Ga}_{\text{Sb}}^{2-}$	1.77	2.71
$\text{Ga}_{\text{Sb}}^{1-}$	1.50	2.44
$\text{Ga}_{\text{Sb}}^0$	1.37	2.30
$\text{Sb}_{\text{Ga}}^-(T_d)$	1.91	0.97
$\text{Sb}_{\text{Ga}}^{2-}(T_d)$	1.56	0.63
$\text{Sb}_{\text{Ga}}^0(C_{3v})$	2.76	1.83
$\text{Ga}_i^{1+}(T_a)$	1.38	1.85
$\text{Ga}_i^{1+}(T_c)$	1.04	1.50
$\text{Sb}_i^{1+}(T_c)$	4.14	3.68
$\text{Sb}_i^{2+}(T_c)$	3.68	3.21
$\text{Sb}_i^{3+}(T_c)$	3.49	3.02
$\text{Sb}_i^{2+}(T_a)$	4.22	3.75
$\text{Sb}_i^{3+}(T_a)$	3.99	3.52
$\text{Sb}_i^{1+}(H)$	3.78	3.31
$(\text{Sb-Sb})_{\text{Sb}(110)}^{1-}$ <sup>a</sup>	4.68	4.22
$(\text{Sb-Sb})_{\text{Sb}(110)}^0$	3.97	3.51
$(\text{Sb-Sb})_{\text{Sb}(110)}^{1+}$	3.60	3.13

<sup>a</sup>Split-interstitial rotates away from the initial  $\langle 110 \rangle$  orientation.

( $2 - /3 -$ ) ionization level is relatively close to the conduction band minimum (CBM) due to the smaller band gap. However, the LDA calculations by Hakala *et al.*<sup>6</sup> missed the neutral charge state and the ( $0/1 -$ ) ionization level close to VBM. In all the different charge states the Sb atoms neighboring the Ga vacancy relax inwards around 11% of the bond distance conserving the  $T_d$  symmetry. This reflects the rather delocalized nature of the electrons on the Ga vacancy deep levels.

The Sb vacancy is stable in the charge states  $+3$ ,  $+1$ ,  $0$ , and  $-2$ . In comparison to the LDA results<sup>6</sup> the use of the HSE06 functional has stabilized the  $+3$  state and the  $-2$  charge state is now stable instead of the  $-1$  charge state. For the As vacancy in GaAs the HSE06 functional gives also the charge state  $-2$  very close to CBM, but in addition the  $-1$  charge state is stable and the  $+3$  charge state is missing.<sup>23</sup> On the other hand, similar to the present result for the Sb vacancy semilocal functionals give the negative-U transition ( $3 + /1 +$ ) for the As vacancy.<sup>11</sup> The relaxation of the Ga atoms around the Sb vacancy depends strongly and rather linearly on the charge state so that the inward relaxation of 23% of the double negative vacancy vanishes for the singly positive vacancy and the relaxation for the triply positive charge state is outwards of 20%. This is a result of the rather localized deep level electrons and the fact that Ga atoms are clearly smaller than the Sb atoms. The localized character is reflected also in the breaking of the  $T_d$  symmetry for the neutral Sb vacancy.

The  $\text{Ga}_{\text{Sb}}$  antisite in GaSb was found to be stable in the charge states from 0 to  $-2$  in agreement with the previous

LDA calculations.<sup>6</sup> For comparison, the HSE06 calculations for the  $\text{Ga}_{\text{As}}$  antisite in GaAs give also the  $+1$  charge state near the VBM.<sup>23</sup> The  $\text{Ga}_{\text{Sb}}$  antisite preserves the  $T_d$  symmetry in all its charge states so that the relaxation is, reflecting the small size of the Ga atom, inwards and rather constant, around 7%.

The  $\text{Sb}_{\text{Ga}}$  antisite in GaSb is stable in the charge states  $+2$  and  $+1$ , with a symmetry-conserving outward relaxation of around 7% of the nearest-neighbor Sb atoms. The existence of the positive charge states is in a striking contrast with the previous LDA calculations which predicted the neutral state as the only stable charge state.<sup>6</sup> The position of the ionization level ( $2+/1+$ ) located at 0.36 eV [i.e., near the middle of the gap resembles the behavior of the HSE06 results for the  $\text{As}_{\text{Ga}}$  antisite in GaAs (Refs. 10,23)]. The HSE06 calculations for GaAs indicate also that the neutral  $\text{As}_{\text{Ga}}$  antisite is stable in the uppermost third of the band gap. Similar results were also found for  $\text{Sb}_{\text{Al}}$  antisite in AlSb in Ref. 12, where charge states from  $+2$  to  $-1$  were found to be stable. We also performed LDA calculations for the  $\text{Sb}_{\text{Ga}}$  antisite, with the same system settings (system size and energy correction term) as with the HSE06 functional. Our LDA results for  $\text{Sb}_{\text{Ga}}$  antisite resembles those of Ref. 6, except that now the  $+1$  charge state is stable with Fermi levels near the valence band edge.

In accordance with semilocal functional calculations for III-V compound semiconductors<sup>11,12,24</sup> our HSE06 calculations predict the existence of a metastable  $C_{3v}$  configuration for the neutral  $\text{Sb}_{\text{Ga}}$  antisite (in GaAs this corresponds to the metastability of the EL2 defect). In the  $C_{3v}$  configuration the Sb atom from the center of the antisite defect has moved 1.56 Å along the [111] direction and penetrated the triangle formed by the three neighboring Sb atoms. The metastable  $C_{3v}$  configuration has only the neutral charge state in the band gap. We have calculated the energy landscape of the neutral  $\text{Sb}_{\text{Ga}}$  antisite with respect to the movement of the central Sb atom along the [111] direction towards the open interstitial position by using the climbing-image nudged elastic band method.<sup>25</sup> The results are shown in Fig. 2. The HSE06 functional calculation gives the metastable  $C_{3v}$  configuration at the same energy as the neutral  $T_d$  configuration. The thermal barrier from the  $T_d$  configuration to the  $C_{3v}$  configuration is 0.25 eV which would allow a high jumping rate already at the room temperature.

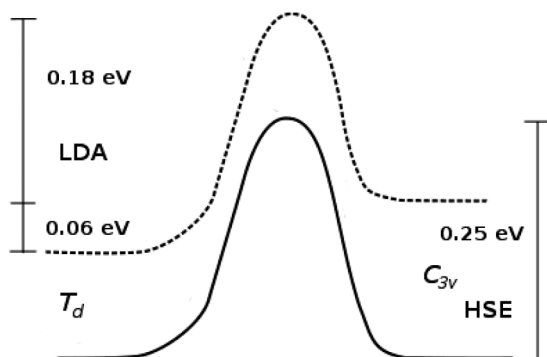


FIG. 2. Schematic illustration of the transformation from the  $T_d$  configuration to the  $C_{3v}$  configuration for the neutral  $\text{Sb}_{\text{Ga}}$  antisite defect. The results of the HSE06 (solid line) and LDA (dashed line) functional calculations are shown.

This differs from the situation for the LDA functional where the  $T_d$  configuration is lower in energy by 0.06 eV and the barrier from the  $C_{3v}$  configuration back to  $T_d$  configuration is only 0.18 eV.

The Ga interstitial is stable only in the  $+1$  charge state and in the tetrahedral configurations  $T_c$  and  $T_a$ . In both configurations there is a symmetry-conserving 5% outwards relaxation. The Sb interstitial exist in all the sites  $T_c$ ,  $T_a$ , and  $H$  having the stable charge states from  $+3$  to  $+1$  at the  $T_c$  site,  $+2$  and  $+1$  at the  $T_a$  site, and the charge state  $+1$  at the  $H$  site. The LDA results by Hakala *et al.*<sup>6</sup> are roughly similar finding the singly positive Ga interstitial in the  $T_c$  site, the triply and singly positive Sb interstitials in the  $T_c$  site, and the singly positive Sb interstitial in the  $H$  site. The semilocal functional results for GaAs indicate that also the doubly and triply positive Ga interstitials are stable.<sup>11</sup> Moreover, those calculations<sup>11</sup> predicted the existence of the singly negative As interstitial in the upper part of the band gap and, parallel to our results for the Sb interstitial, the appearance of the ( $3+/1+$ ) ionization level.

The Sb split-interstitial is stable in the  $+1$ ,  $0$ , and  $-1$  charge states. In the  $+1$  and  $0$  charge states the Sb split-interstitial remains oriented along the initial  $\langle 110 \rangle$  direction, but in the  $-1$  charge state it rotates away from it. This is in contrast to AlSb where the  $(\text{Sb-Sb})_{\text{Sb}(110)}$  split-interstitial was found to be stable in all the charge states from  $+2$  to  $-2$  (Ref. 19) and remain oriented along the  $\langle 110 \rangle$  direction in all charge states. According to the Table I the formation energy of the  $(\text{Sb-Sb})_{\text{Sb}(110)}$  split-interstitial is also rather high in GaSb.

## B. Formation energies of native point defects in different growth conditions

Figures 3(a) and 3(b) give the formation energies for most important point defects in GaSb as a function of the Fermi level in Ga-rich and Sb-rich growth conditions, respectively. The figures are based on the numerical data in Table I. The formation energies of the Sb interstitials and  $(\text{Sb-Sb})_{\text{Sb}(110)}$  split-interstitials are considerably high when compared to the other defects and, therefore, as thermodynamically unlikely defects they are not shown.

In the Ga-rich growth conditions the defects with the lowest formation energies are the  $\text{Ga}_i^{1+}(T_c)$  interstitial and the  $\text{Ga}_{\text{Sb}}^{2-}$  antisite. Moving to the Sb-rich growth conditions turns the  $\text{Sb}_{\text{Ga}}$  antisite into the most favorable defect with the exception of the region very close to the CBM. Moreover, the formation energy of the Ga vacancy decreases and that of the  $\text{Ga}_i^{1+}(T_c)$  interstitial increases.

In general our HSE06 functional results show characteristics similar to those by Hakala *et al.*<sup>6</sup> obtained by using the LDA although the present formation energies are clearly larger. For example, the formation energies of Ga and Sb vacancies have raised by roughly 1 eV. The main qualitative difference with respect to the previous LDA results<sup>6</sup> is, however, that hybrid functionals favor more positive charge states. This trend was found also in the case of oxygen vacancies in transparent conducting oxides by Ágoston *et al.*<sup>26</sup> and it reflects mainly the relative lowering of the valence band states due to the reduction in the spurious electron self-interaction. Most notably, this makes the positive charge states of the  $\text{Sb}_{\text{Ga}}$  antisite stable and

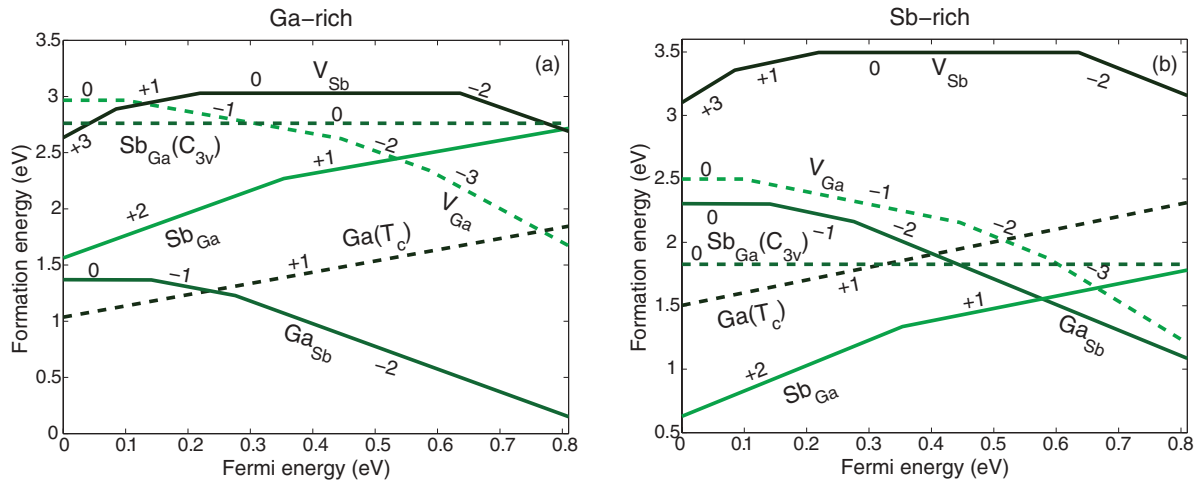


FIG. 3. (Color online) Formation energies for stable charge states of point defects in GaSb as a function of the Fermi level in (a) Ga-rich and (b) Sb-rich growth conditions.

causes the appearance of the donor level (2 + /1 +) in the band gap at 0.36 eV above the VBM.

We have also performed most of the calculations using LDA with the same system settings as with the HSE06 functional. The LDA results are rather similar to the results in Ref. 6 and thus the qualitative differences between our HSE06 results and those of Ref. 6 cannot be explained by differences in computational details, but reflect the differences between the different functionals used.

C. Extrinsic point defects C<sub>Sb</sub> and O(T<sub>c</sub>)

Figure 4 shows the formation energies for substitutional carbon C<sub>Sb</sub> and interstitial oxygen O(T<sub>c</sub>) as a function of the Fermi level. C<sub>Sb</sub> is in the singly negative charge state for the whole range of the Fermi level similarly to AlSb (Ref. 13). The C<sub>Sb</sub> remains in the T<sub>d</sub> symmetry during relaxation. Interstitial oxygen in the T<sub>c</sub> site has stable charge states -1

and -2 in the gap and the ionization level (-1/ -2) is located at 0.29 eV. The O(T<sub>c</sub>) has the C<sub>3v</sub> symmetry at the -1 charge state and T<sub>d</sub> symmetry at the -2 charge state. Both C<sub>Sb</sub> and O(T<sub>c</sub>) act as acceptors for the whole range of the Fermi level and can thus trap excess electrons and contribute to the p-type conductivity. According to Fig. 4 the formation energy of the C<sub>Sb</sub> is very high compared to that of O(T<sub>c</sub>) and thus the oxygen would clearly be a much more likely candidate to compensate the possible donor character of the Sb<sub>Ga</sub> antisite.

IV. DISCUSSION: p-TYPE CONDUCTIVITY OF UNDOPED GaSb

The very reasonable qualitative agreement of our HSE06 functional results with the previous semilocal functional results for defects in GaSb and GaAs and with the HSE06 results for defects in GaAs gives credence to our discussion about the origin of the p-type conductivity of GaSb.

According to Fig. 3, the Ga<sub>Sb</sub> antisite acts as a single and as a double acceptor for Fermi levels above 0.13 and 0.27 eV, respectively. Thus, in Ga-rich growth conditions the most likely source of p-type conductivity are the Ga<sub>Sb</sub><sup>2-</sup> antisites. Compensation due to the Ga<sub>i</sub><sup>1+</sup>(T<sub>c</sub>) interstitials is not expected because of their high mobility and recombination with open volume defects already below the room temperature. When going from Ga-rich to Sb-rich growth conditions the formation energy of the Ga<sub>Sb</sub> antisite increases considerably predicting a decrease in the p-type conductivity. This has actually been observed in experiments<sup>27</sup> where a significant drop in the number of background acceptors was observed.

Especially in Sb-rich growth conditions the formation energy of the Sb<sub>Ga</sub> antisite is notably low. It is a single or even a double donor over the whole range of the Fermi level in the band gap and its existence would make GaSb n-type when the growth stoichiometry turns to the Sb-rich side. One possible explanation to this apparent discrepancy could be the turning of the T<sub>d</sub> configuration of the Sb<sub>Ga</sub> antisite to the C<sub>3v</sub> configuration. The latter configuration is neutral for all the Fermi level positions. Given the accuracy of our calculations as reflected also in the magnitude and

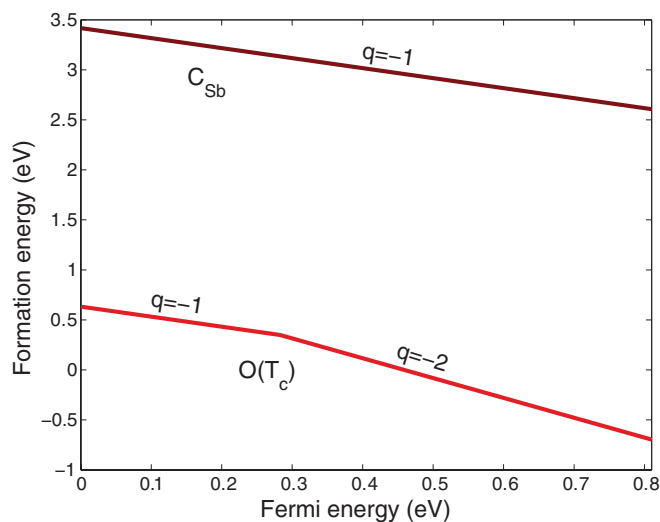


FIG. 4. (Color online) Formation energies for extrinsic impurity defects C<sub>Sb</sub> and O(T<sub>c</sub>) as a function of the Fermi level in Sb-rich growth conditions.

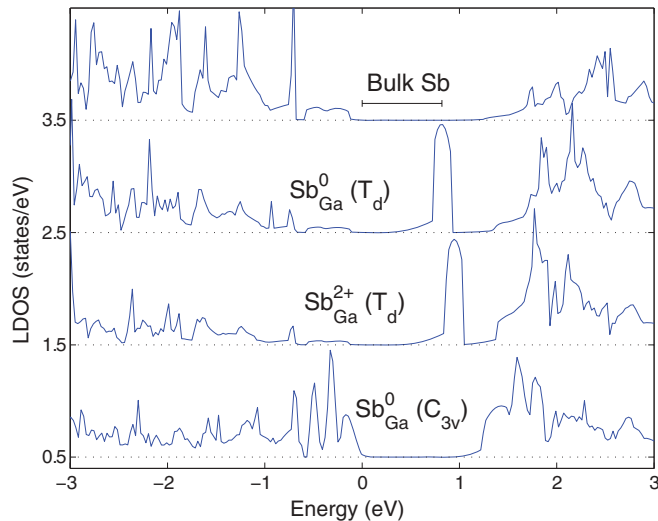


FIG. 5. (Color online) LDOS for the Sb atom in bulk GaSb and in the defect systems. The LDOS shown for the defect systems correspond to the defect atom. The energy zero coincides with the top of the valence band at the  $\Gamma$  point. The original zero LDOS values of the adjacent curves given by horizontal dashed lines are shifted relative to each other. The solid segment at the topmost LDOS curve indicates the band gap in bulk GaSb.

trend in the difference between the LDA and HSE06 results in Fig. 2 above, the actual situation could be that the neutral  $C_{3v}$  configuration is energetically favored and easily reachable by thermal excitation from the neutral  $T_d$  configuration. The neutral  $T_d$  configuration could result when the strong and narrow resonance at the CBM seen in the LDOS of the  $Sb_{Ga}^{2+}$  in Fig. 5 for the  $T_d$  configuration captures electrons from the conduction band.

In addition to the above over-the-thermal-barrier route the  $C_{3v}$  configuration could be also reached from the neutral  $T_d$  configuration by photoexcitation according to the model proposed by Dabrowski and Scheffler<sup>28</sup> for the EL2 defect in GaAs. In this model a resonance level in the conduction band induced by the  $As_{Ga}$  antisite is occupied due to (photo) excitation from the deep level in the band gap and then the defect relaxes spontaneously to the metastable  $C_{3v}$  configuration. Indeed the LDOS in Fig. 5 shows that also the  $Sb_{Ga}$  antisite induces rather localized states at about 1.8 eV above the VBM. The strong resonance just above the CBM, which was discussed above, corresponds to the deep gap state of the EL2 defect in GaAs. According to partial charge densities the character of the resonance states at about 1.8 eV agree with the Dabrowski-Scheffler model. Moreover, as shown in Fig 5, in the  $C_{3v}$  configuration there are resonance states just below the VBM. These correspond to the level found by Dabrowski and Scheffler in the band gap just above the VBM. Thus, we

propose the model that electrons excited to the conduction band are captured effectively by the resonance induced by the positive antisite close to the CBM. A further photoexcitation of the captured electrons to the resonance states at about 1.8 eV above the VBM results in the relaxation to the  $C_{3v}$  configuration in accordance with the Dabrowski-Scheffler model. The resonances induced by the neutral  $C_{3v}$  defect are relatively far from the band gap and thus less localized than those induced by the Sb antisite and therefore they are expected to be less active in electron capture of photoexcitation processes.

Another explanation to  $p$ -type conductivity in the Sb-rich growth conditions are the extrinsic point defects, namely, carbon in the substitutional Sb site and oxygen in the interstitial cation site. Indeed, according to our calculations the formation energy for the oxygen interstitial is very low. These defects act as acceptors and could compensate the donor character of the  $Sb_{Ga}$  antisite. However, to our knowledge undoped GaSb is always  $p$ -type regardless of the method of the growth suggesting that the extrinsic defects are not crucial for the  $p$ -type conductivity of GaSb.

## V. CONCLUSION

We have studied native point defects in GaSb within the DFT framework. The use of the hybrid exchange-correlation functional was found to affect crucially the important relative energetics of the different defects. The lowest-energy defects found are the Ga antisite, the Ga interstitials, and the Sb antisite. Especially, the formation energy of the  $Ga_{Sb}^{2-}$  antisite was predicted to be considerably low in Ga-rich growth conditions and thus the source of the  $p$ -type conductivity. However, in contrast to earlier LDA studies also the formation energy of the Sb antisite was found to be considerably low in Sb-rich growth conditions. This is due to the positive charge states stabilized by the hybrid functional. The existence of the positive charge states means also that the Sb antisite should act as a donor in Sb-rich growth conditions contributing to  $n$ -type conductivity (or the efficient compensation of the  $p$ -type conductivity), which is not observed in the experiments. As a solution to this discrepancy we studied the metastability of the Sb antisite. In addition we found that extrinsic point defects  $C_{Sb}$  and  $O(T_c)$  act as acceptors in GaSb and especially  $O(T_c)$ , having a low formation energy, might compensate the electrical activity of the  $Sb_{Ga}$  antisite.

## ACKNOWLEDGMENTS

This work has been supported by the Academy of Finland through the Center of Excellence program. The computer time was provided by the Finnish IT Center for Science and Technology (CSC).

<sup>1</sup>P. S. Dutta, H. L. Bhat, and V. Kumar, *J. Appl. Phys.* **81**, 5821 (1997).

<sup>2</sup>J. Paaajaste, S. Suomalainen, R. Koskinen, A. Härkönen, M. Guina, and M. Pessa, *J. Cryst. Growth* **311**, 1917 (2009).

<sup>3</sup>D. Wang, S. P. Svensson, L. Shterengas, G. Belenky, C. S. Kim, I. Vurgaftman, and J. R. Meyer, *J. Appl. Phys.* **105**, 014904 (2009).

<sup>4</sup>V. Virkkala, V. Havu, F. Tuomisto, and M. J. Puska, *Phys. Rev. B* **85**, 085134 (2012).

- <sup>5</sup>C. C. Ling, M. K. Lui, S. K. Ma, X. D. Chen, S. Fung, and C. D. Beling, *Appl. Phys. Lett.* **85**, 384 (2004).
- <sup>6</sup>M. Hakala, M. J. Puska, and R. M. Nieminen, *J. Appl. Phys.* **91**, 4988 (2002).
- <sup>7</sup>A. Peles, A. Janotti, and C. G. Van de Walle, *Phys. Rev. B* **78**, 035204 (2008).
- <sup>8</sup>R. M. Nieminen, *Modell. Simul. Mater. Sci. Eng.* **17**, 084001 (2009).
- <sup>9</sup>C. Freysoldt, J. Neugebauer, and C. G. Van de Walle, *Phys. Status Solidi B* **248**, 1067 (2010).
- <sup>10</sup>H.-P. Komsa and A. Pasquarello, *Phys. Rev. B* **84**, 075207 (2011).
- <sup>11</sup>P. A. Schultz and O. A. von Lilienfeld, *Modell. Simul. Mater. Sci. Eng.* **17**, 084007 (2009).
- <sup>12</sup>M.-H. Du, *Phys. Rev. B* **79**, 045207 (2009).
- <sup>13</sup>P. Erhart, D. Åberg, and V. Lordi, *Phys. Rev. B* **81**, 195216 (2010).
- <sup>14</sup>G. Kresse and J. Furthmüller, *Comput. Mater. Sci.* **6**, 15 (1996).
- <sup>15</sup>G. Kresse and D. Joubert, *Phys. Rev. B* **59**, 1758 (1999).
- <sup>16</sup>J. Heyd, J. E. Peralta, G. E. Scuseria, and R. L. Martin, *J. Chem. Phys.* **123**, 174101 (2005).
- <sup>17</sup>L. S. dos Santos, W. G. Schmidt, and E. Rauls, *Phys. Rev. B* **84**, 115201 (2011).
- <sup>18</sup>I. Vurgaftman, J. R. Meyer, and L. R. Ram-Mohan, *J. Appl. Phys.* **89**, 5815 (2001).
- <sup>19</sup>D. Åberg, P. Erhart, A. J. Williamson, and V. Lordi, *Phys. Rev. B* **77**, 165206 (2008).
- <sup>20</sup>*Ternary and Quaternary A<sub>3</sub>B<sub>5</sub> Semiconductors in Handbook Series on Semiconductor Parameters*, edited by M. Levinshtein, S. Rumyantsev, and M. Shur (World Scientific, Singapore, 1999), Vol. 2.
- <sup>21</sup>C. G. Van de Walle and J. Neugebauer, *J. Appl. Phys.* **95**, 3851 (2004).
- <sup>22</sup>D. D. Wagman, W. H. Evans, V. B. Parker, R. H. Schumm, I. Halow, S. M. Bailey, K. L. Churney, and R. L. Nuttal, *J. Phys. Chem. Ref. Data* **11**, Supplement 2 (1982).
- <sup>23</sup>H.-P. Komsa and A. Pasquarello, *J. Phys.: Condens. Matter* **24**, 045801 (2012).
- <sup>24</sup>M. J. Caldas, J. Dabrowski, A. Fazzio, and M. Scheffler, *Phys. Rev. Lett.* **65**, 2046 (1990).
- <sup>25</sup>G. Henkelman and H. Jónsson, *J. Chem. Phys.* **113**, 9978 (2000).
- <sup>26</sup>P. Ágoston, K. Albe, R. M. Nieminen, and M. J. Puska, *Phys. Rev. Lett.* **103**, 245501 (2009).
- <sup>27</sup>Y. J. Van der Meulen, *J. Phys. Chem. Solids* **28**, 25 (1967).
- <sup>28</sup>J. Dabrowski and M. Scheffler, *Phys. Rev. Lett.* **60**, 2183 (1988).